

NUMERICAL AND EXPERIMENTAL DEFORMATION AND FAILURE ANALYSIS OF 3D-TEXTILE REINFORCED LIGHTWEIGHT STRUCTURES UNDER IMPACT LOADS

Werner Hufenbach, Maik Gude, Andreas Hornig*, Robert Böhm, Matthias Zscheuye

Institut für Leichtbau und Kunststofftechnik (ILK), TU Dresden
01062 Dresden, Germany
*Andreas.Hornig@tu-dresden.de

ABSTRACT

The paper deals with the predictive modelling of a complex shaped 3D-textile reinforced laminate structures under impact loading conditions. The model's capabilities to predict the deformation behaviour have been investigated using a bucket structure for bulk goods transportation as an example.

The reinforcement structure of the bucket consists of a novel multi-layered flat bed weft knitted textile preform. A drop tower with spherically shaped impactors were used for various impact experiments, where the impact energy as well as the loading direction and the impact location have been varied. The experimental setup allows the examination of the real time deformation behaviour from different perspectives via two high speed video cameras.

The numerical investigations were focused on the realistic prediction of the impact behaviour in terms of the elastic structural deformation during the impact, failure and the post impact damage behaviour. Therefore complex failure models for composites based on HASHIN, the damage model based on MATZENMILLER and an approach for strain rate dependency were applied by the use of *MAT_COMPOSITE_DMG_MSC in LS-DYNA.

It has been shown that material characteristic properties and the material model enable a realistic prediction of the experimentally observable deformation, impact damage and failure phenomena of complex shaped 3D-reinforced composite structures.

1. INTRODUCTION

Fibre and textile reinforced composites have firmed their position as lightweight materials, which can be specifically customised in terms of their material properties for particular loading conditions. With careful tailoring, textile reinforced composite structures provide considerable advantages concerning weight optimisation and structural stiffness, especially for applications which have to account for highly dynamic crash and impact loading conditions [1]. In this respect, 2D-textile reinforced composites became standard not only for modern structural aircraft applications, but also for a broad range of engineering applications.

The conducted study deals with the emerging trend of using 3D-textile reinforced materials in conventional fields of mechanical engineering and construction applications under consideration of the design and optimisation process [2]. 3D-textile reinforced composites are commonly considered to enhance the through-the-thickness properties, such as interlaminar shear and normal strength, damage tolerance and fracture toughness. Particularly relevant in the structural design process is to enhance the delamination resistance. The recently invented multi-layered flat bed weft knitting technique (MKF) is a well suited possibility to realise such a spatial reinforced material [3]. In addition to the advanced mechanical performance, the MKF offers advanced drapability and near net shape manufacturing capabilities [4], [5].

The load-adapted and optimised design of 3D-textile reinforced composites for crash and impact applications requires an assured knowledge of the strain rate dependent deformation and failure behaviour [1]. In addition, an efficient design of composite

structures for applications under impact loads strongly depends on numerical reliable and sufficiently accurate material models [6].

The fundamental understanding of the material behaviour and its properties under consideration of phenomenological failure approaches have to be transferred into a Finite Element (FE)-System [7]. One of the challenging tasks of structural design issues for such 3D textile reinforced composites is the predictive modelling of failure under complex loading conditions in order to overcome expensive material and structural testing especially for crash and impact applications [2].

The solid orthotropic damage model for fibre reinforced composites MAT161/162 in LS-DYNA has been chosen and validated for the numerical work, since it provides reasonable phenomenological approaches. A modified HASHIN [8] failure criterion is available for in-plane load failure and a shear and normal stress based delamination criterion for out-of-plane failure treatment. Additionally, the used damage model is based on MATZENMILLER [9] and the strain rate dependency is taken into account.

2. 3D-REINFORCED COMPOSITE STRUCTURE

The investigated bucket structure for conveying machinery can be seen as an appropriate example for application oriented investigations. Due to the high importance of weight reduction in energy efficient conveying machinery, the complex shaped geometry and its static and dynamic loading case conditions, the bucket is predestined as a demonstrator structure for the continuous lightweight design process. The reinforcement structure of the bucket consists of a near net shape knitted glass fiber textile preform, which has been infiltrated in a resin transfer (RTM) process (Figure 1) [5]. The epoxy matrix resin system RIM 135 with RIMH 134-137 hardener was used for the infiltration process.

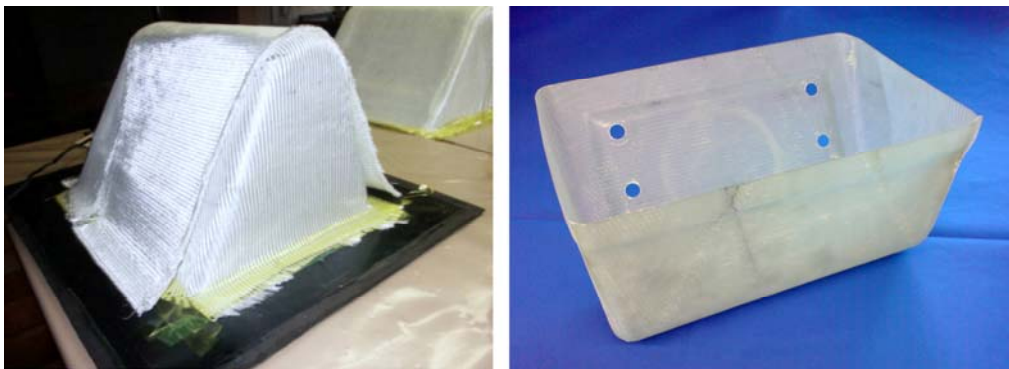


Figure 1: Bucket composite structure, left: perform in the RTM moulding tool, right: infiltrated and machined structure [5]

A 3D reinforced material, the multi-layered weft knitted fabric (MKF), was used for the textile perform and has been developed and fabricated by the Institut für Textil- und Bekleidungstechnik (ITB), TU Dresden [3], [4]. Multiple configurations of the MKF are available, whereas the type 1b as illustrated in Figure 2 has been used for the bucket structure. It is composed of glass fibers, where the weft (1200 tex) and warp yarn (2400 tex) are held together by a stitching yarn (137 tex). The stitch density of the weft yarn differs to the warp yarn, which results in mass fraction of 50 % in each of the two reinforcement directions. The perform lay-up corresponds to two symmetrically arranged layers at the main parts ([90/0//0/90]) and one layer ([90/0]) at the side parts of the bucked-structure.

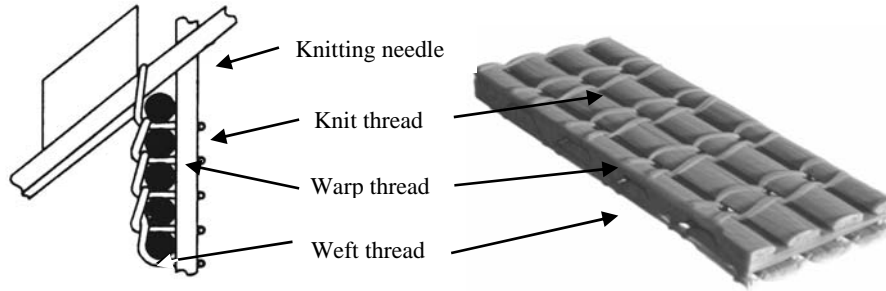


Figure 2: MKF type 1b, left: basic architecture (schematic) [3], right: CT-scan of two symmetrically arranged layers [7]

3. IMPACT LOADING CASE SCENARIOS

Three fundamental impact loading cases (LC 1-3, Figure 3) have been identified representing the worst case impact scenarios in the structure. Transporting boulder or single stones can hit the bucket with varying impact positions and impact angles β_{imp} . In each case the impactor is being represented by a metallic sphere.

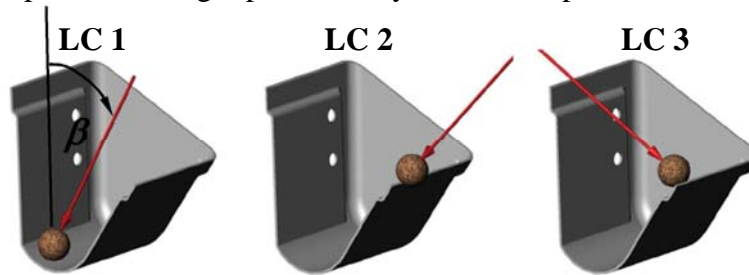


Figure 3 Definition of the impact loading case (LC) scenarios

Additionally, different impactor configurations have been applied, each varying in the initial velocity v_{imp} , impactor mass m_{imp} and therefore different kinetic energies E_{kin} (Table 1) resulting in five impact experiment scenarios.

Table 1: Specification of the impact loading case (LC) scenarios

	impactor				
	v_{imp} [m/s]	m_{imp} [kg]	position	β_{imp} [°]	E_{kin} [J]
LC 1	5,5	0,5	bottom, central	35	7,56
LC 2	5	0,5	leading edge, central	45	6,25
LC 3	3	0,5	leading edge, central	-125	2,25
LC 1-a	8	4	bottom, central	35	128
LC 1-b	8	0,5	bottom, central	35	16

4. NUMERICAL IMPACT ANALYSIS

The numerical investigations were focused on the realistic prediction of the impact behaviour in terms of the elastic deformation during the impact and the post impact damage behaviour. Therefore, complex failure models for composites based on HASHIN [8], the damage model based on MATZENMILLER [9] and an approach for strain rate dependency were applied by the useage of *MAT_COMPOSITE_DMG_MSC (MAT

162) in LS-DYNA. The required strain rate dependent material properties have been determined in highly dynamic tension, compression and shear tests [10].

4.1 PHENOMENOLOGICAL BACKGROUND

Failure model

The failure mechanisms have been investigated with a model based on HASHIN [8], offering models for unidirectional reinforcements (UD-model) and plain weave reinforcements (BD-model). The failure criterion can be described in stress [11] or strain based [12] formulations. Extensive investigations showed, that the actually implemented criteria vary in their formulations. However, with the focus on the phenomenological understanding, the presented criteria are all expressed as stress based formulations.

It is important to point out that a main focus of the numerical investigations was a predictive modelling approach by basic material tests on the material level (parameter identification) in a first stage and validation tests on a structural level (model validation) in a second stage. Especially the results of the dynamic elastic response, as explained in 6.1, followed strictly this approach. In terms of failure prediction, the UD-model could be validated best by the experiments. The results indicated that the BD-model cannot represent the occurrence of inter-fiber-failure in MKF (Figure 2) satisfyingly.

The UD-failure model will be described in the following. Three basic types of fiber failure can be evaluated:

- fiber tension and fiber shear failure:

$$\left(\frac{\langle \sigma_1 \rangle}{R_1'} \right)^2 + \left(\frac{\tau_{21}^2 + \tau_{31}^2}{R_{FS}^2} \right) \geq 1 \quad (1)$$

with the MACAULAY brackets: $\langle x \rangle = \frac{|x| + x}{2}$

- fiber compression failure:

$$\left(\frac{\langle \sigma_1' \rangle}{R_1^c} \right)^2 \geq 1 \quad \text{with } \sigma_1' = -\sigma_1 + \langle -\sigma_3 \rangle \quad (2)$$

- and fiber crushing:

$$\left(\frac{\langle p \rangle}{R_{FC}} \right)^2 \geq 1 \quad , \quad p = -\frac{(\sigma_1 + \sigma_2 + \sigma_3)}{3} \quad (3)$$

with σ and τ denoting the stresses in fiber (1), transverse (2) and through thickness direction (3) of the laminate according to Figure 4. R denotes the strength with the indices t and c for tension and compression, FS for fiber shear and FC for fiber crushing.

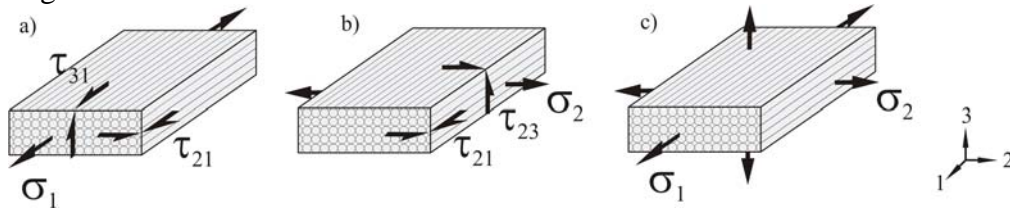


Figure 4 Fiber failure relevant stresses for a) fiber tension, b) fiber shear and c) fiber compression and crushing failure

Matrix or inter-fiber failure is treated independently of the fiber failure modes (Figure 5) and is represented by

- matrix failure perpendicular to the 1-2-plane (inter-fiber failure)

$$\left\{ \left(\frac{\langle \sigma_2 \rangle}{R_2^d} \right)^2 + \left(\frac{\tau_{21}}{R_{21} + \tan \alpha \langle -\sigma_2 \rangle} \right)^2 + \left(\frac{\tau_{23}}{R_{23} + \tan \alpha \langle -\sigma_2 \rangle} \right)^2 \right\} \geq 1 \quad (4)$$

- matrix failure parallel to the 1-2-plane (delamination)

$$s^2 \left\{ \left(\frac{\langle \sigma_3 \rangle}{R_3^d} \right)^2 + \left(\frac{\tau_{23}}{R_{23} + \tan \alpha \langle -\sigma_3 \rangle} \right)^2 + \left(\frac{\tau_{31}}{R_{13} + \tan \alpha \langle -\sigma_3 \rangle} \right)^2 \right\} \geq 1 \quad (5)$$

Compression stresses, which influence the failure mechanisms, are taken into account by the MOHR-COULOMB's idea of internal friction and the corresponding friction angle α . The additional delamination factor s in the delamination criterion eq. (5) allows to represent stress concentrations at the delamination crack tip. The initial value is set to 1 and in the case of element delamination, s will be reduced to a predefined value in the surrounding elements in order to model delamination propagation more adequately.

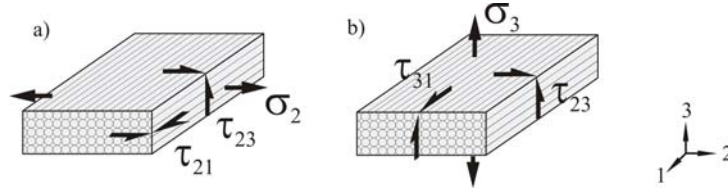


Figure 5 Matrix failure relevant stresses for matrix failure a) perpendicular to the 1-2-plane and b) parallel to the 1-2-plane (delamination)

Damage model

The damage specific variable ω_i for the stiffness degradation of E_i in the damage model in MAT 162 [12] can be expressed as

$$\omega_i = 1 - e^{\frac{1}{m_k}(1-r_j^{m_k})} \quad \text{for } r_j \geq 1 \quad (6)$$

with r_j representing the damage threshold of each independent damage criterion (1...5, eq. (1)-(5)) and m_k the material specific damage softening coefficient for stiffness degradation ($k = 1...3$, fiber failure, matrix failure and fiber crushing). Subsequently, the stiffness degradation is calculated by

$$E'_i = (1 - \omega_i) E_i \quad \text{with } (E'_i)^T = [E'_1, E'_2, E'_3, G'_{12}, G'_{13}, G'_{23}] \quad (7)$$

Strain rate dependency

Many composite materials are exposed to a distinctive strain rate dependency [10] affecting predominantly the strength and stiffness properties. In the used model this relations are expressed for the strength according to

$$R_i(\dot{\epsilon}) = R_i^{ref} \left(1 + A^R \ln \frac{\dot{\epsilon}_i}{\dot{\epsilon}_i^{ref}} \right) \quad (8)$$

and for the stiffness by

$$E_i(\dot{\epsilon}) = E_i^{ref} \left(1 + A_i^E \ln \frac{\dot{\epsilon}_i}{\dot{\epsilon}_i^{ref}} \right) \quad (9)$$

The initial values R_i and E_i are determined for the current state of strain rate $\dot{\epsilon}$ with respect to experimentally obtained reference values R_i^{ref} , E_i^{ref} and $\dot{\epsilon}_i^{ref}$. Material specific coefficients (A^R and A_i^E) are determining the amount of scaling. The coefficient for strength A^R is treated direction independently, which is one of weakness of the model, whereas strain rate stiffness coefficient A_i^R has 6 independent values ($i = 1...6$)

for each stiffness.

4.2 MODEL DEVELOPMENT

As described in chapter 2, the preform-design results in areas with varying layup and material definitions (Figure 6). For such thin laminated structures, shell elements would be the element definition of choice. Instead, eight node brick element (4 elements through the thickness) with one integration point have been used in order to perform a full 3D-failure analysis due to the highly localised energy induction in the impact area. The selective modelling approach in will give an overview of concepts to reduce the high numerical effort without losing the 3D failure information.

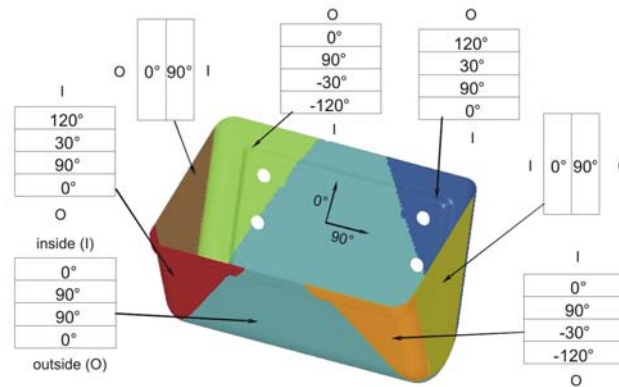


Figure 6 Varying layup in the composite structure

Besides the already mentioned section-wise layup definition, two different material models for eight node volume elements have been used within the explicit solution in LS-DYNA: in the impact area `*MAT_COMPOSITE_DMG_MSC` (MAT 162) (3.1) and `*MAT_ORTHOTROPIC/ ANISOTROPIC_ELASTIC` (`*MAT_002`) in the expected elastically responding part of the structure. The impactor was modelled using `*MAT_ELASTIC` (`*MAT_001`) with an initial velocity definition. Additional boundary conditions have been defined in the clamping area by constraining the nodes. Damping was not considered.

4.3 OPTIMISATION AND SELECTIVE MODELLING

For the evaluation of the occurring failure in the impact area, including failure in laminate through thickness (3-direction), it is mandatory to analyse the 3D stress state, since failure like delamination and the existence of the 3D-reinforcement may affect the results. Using eight node volume elements with four elements through the thickness (one per idealised UD-layer) results in a considerable numerical effort. Therefore, three selective modelling approaches, linking the volume elements of the failure critical impact area with four node shell elements of the remaining areas of the structure have been investigated and compared: constrained nodes (`CONSTRAINED_SHELL_TO_SOLID`), contact definition (`CONTACT_TIED_SHELL_EDGE_TO_SURFACE`) and shared nodes.

In terms of the pre-processing effort, especially the constrained nodes approach results in a considerable additional modelling work, due to the lack of appropriate commercial tools. The possibility of combining varying mesh densities also can be provided by using a contact definition and is therefore the optimisation approach of choice in this study. The numerical effort in terms of the number of elements could be reduced by factor 0.43 and in terms of the calculation time by 0.5.

5. EXPERIMENTAL SETUP AND EQUIPMENT

For the experimental investigations a drop tower has been designed, which allows to adjust to the different impact loading angles as well as the drop heights (max. 5 m) with a surrounding Plexiglas protection (Figure 7).

The impact test was recorded by two high speed video cameras type Phantom[®], allowing a frame rate of up to 11500 frames/s (Figure 7). In the case of the performed low velocity impacts a frame rate of 4000 frames/s was used, which results in a resolution of 800×600. The impactor is held by an electro magnet. The video recording is started automatically by a trigger signal when the impactor is released. The experimental setup also contains two data acquisition laptops for video setup and recording as well as multiple illumination devices as shown in Figure 7.

The deflections during the impacts are recorded via image and pixel correlation respectively and can be directly related to the impact time history. This information were then used to compare the experimentally and numerically determined structural response of the bucket. Additionally, visual inspections have been performed to assess the amount and type of failure.

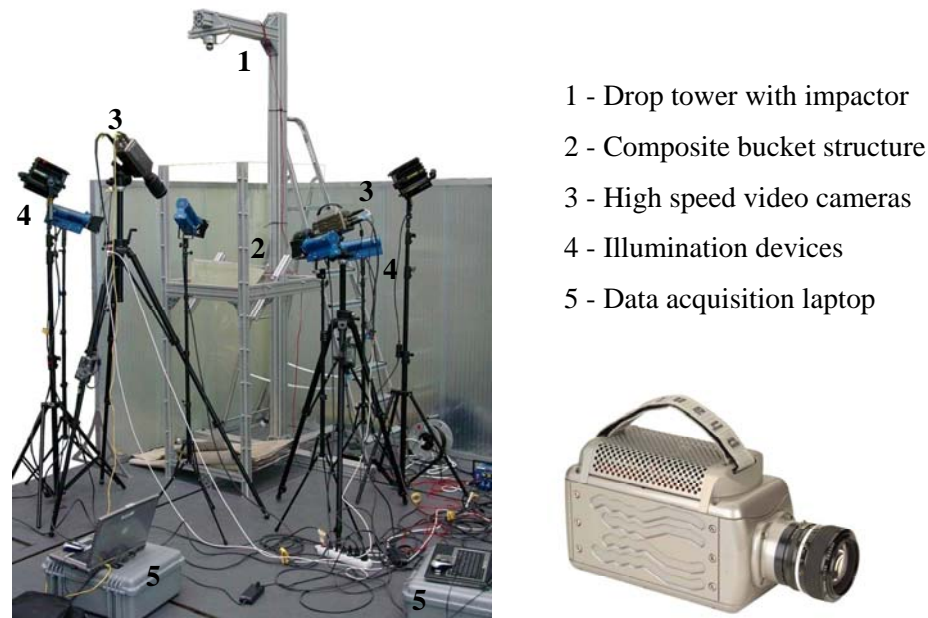


Figure 7 Experimental setup of the impact drop tower with impactor and bucket (left) and the video camera type Phantom[®] (right, source: MAK Bildtechnik)

6. COMPARISON OF THE NUMERICAL PREDICTION AND EXPERIMENTS

The experimental deformation analysis has been performed via image correlation of the high speed video system. In the following, these information have been used for the model validation by comparing numerical predictions and experimental results [13].

As an example, LC 3 is chosen to illustrate the impact test in detail (Figure 8). In this case, 4 stages of global structural elastic response can be identified: a) first contact, b) maximum deflection, c) impactor acceleration and refraction and d) post impact, impactor release and maximum spring-back deformation.

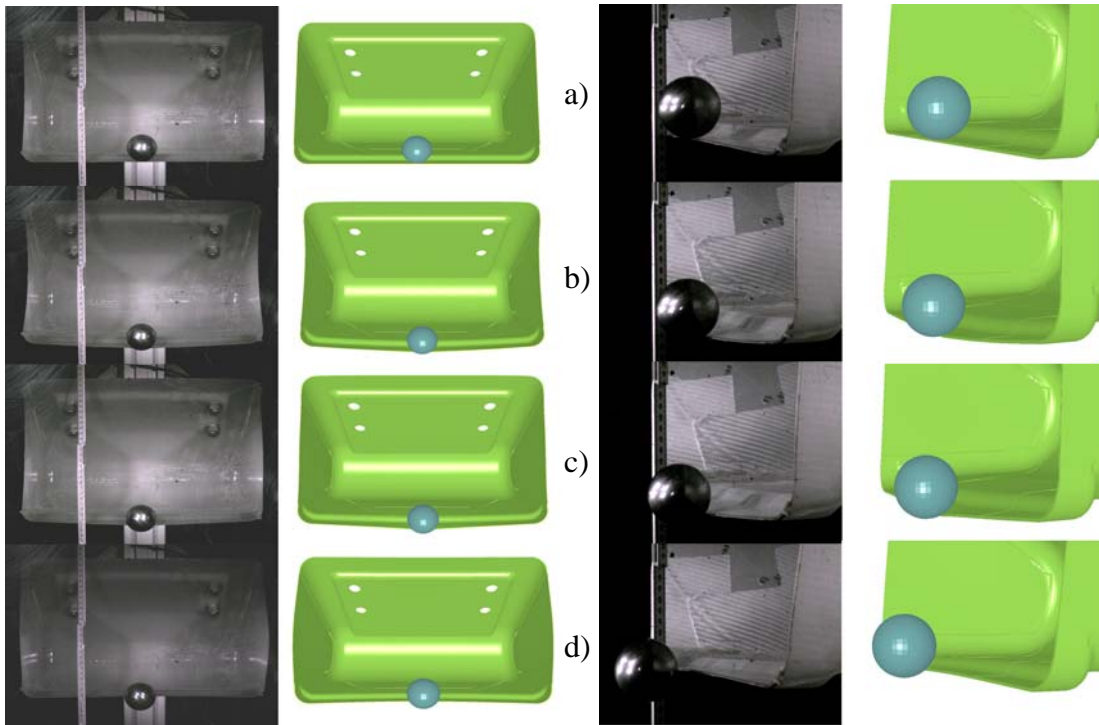
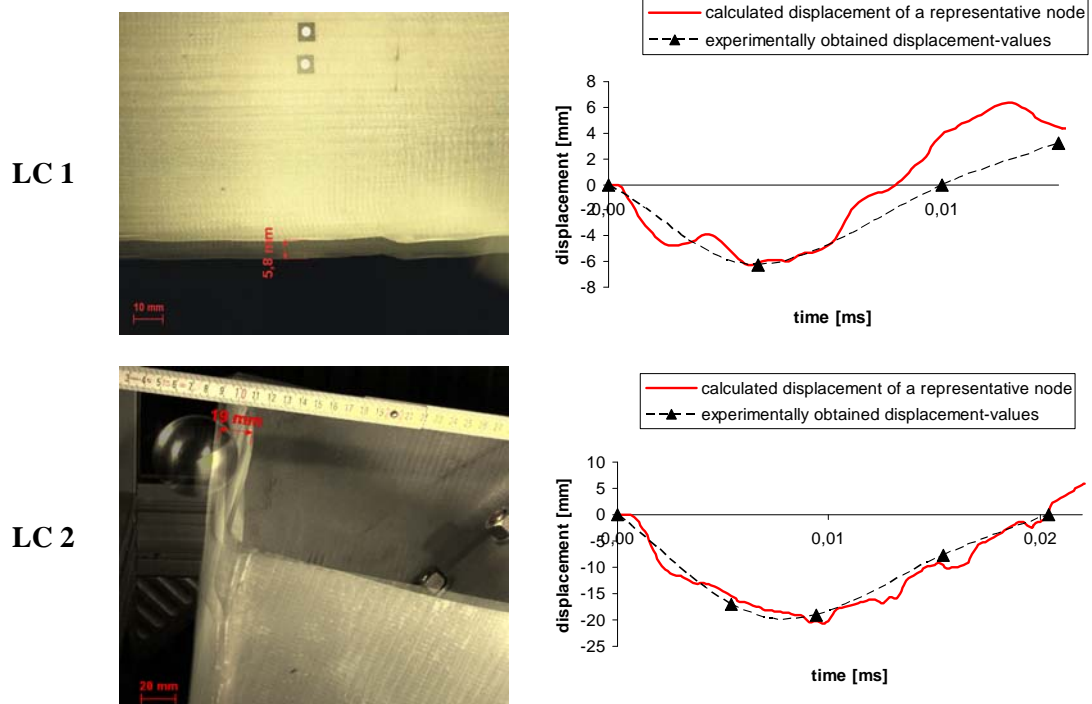


Figure 8 Comparison of the calculated and experimentally obtained elastic response in LC 3:
a) $t_a=0$ (first contact), b) $t_b=9,4$ ms (max. deflection) c) $t_c=14$ ms (impactor acceleration and refraction) and d) $t_d=27$ ms (post contact)

In the first impact period (Figure 8 a-b), the leading edge is deformed until it reaches the maximum deflection ($v_{imp} = 0$ m/s, $E_{kin} = 0$ J, Figure 9) and the side panels deflect inwards. The elastic spring-back forces the impactor to accelerate again and to refract app. 90° with respect to the initial impact angle (Figure 8 c-d).

The local maximum and time dependent deflections are displayed and compared in Figure 9. The numerical and experimental results show a good agreement.



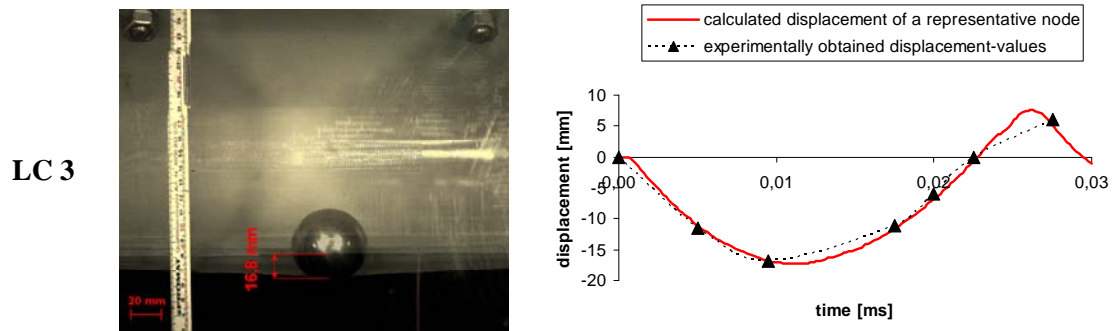


Figure 9 Experimental maximum deflections of LC 1-3 (left) and comparison of the local deflections vs. time during the impact (right)

By comparing the global elastic response (Figure 8) as well as the local displacements (Figure 9) of the loading cases it could be shown, that the numerical and the experimental results and phases correlate very well. Neglecting material damping effects and manufacturing defects may explain the variation in the post impact phase representing the post-oscillation of LC1, where the numerical predictions are conservative and too high.

As illustrated in Figure 10, only a small area of damage has been caused by the impact according to LC 1 – 3, where only inter-fiber failure has been identified (red areas). The location and area in the impact area are represented very accurately allowing to numerically pre-estimate the structural failure behavior of the composite structure.

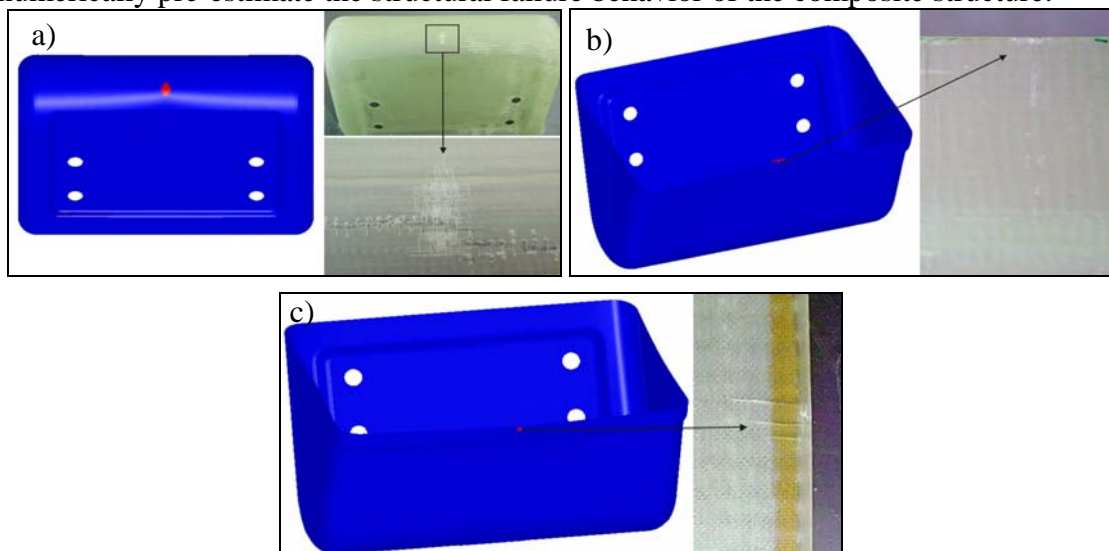


Figure 10 Comparison of the experimentally and numerically obtained failure for a) LC 1, b) LC 2, c) LC 3

7. CONCLUSIONS

The main focus of the presented work was the predictive modelling of failure in composite structures. Due to extensive investigations in terms of the experimental determination of material properties a priori [10] and the fundamental understanding of the material behaviour [2], the governing phenomena have been transferred into a commercially available material model in LS-DYNA and enabled a quantitative and qualitative evaluation of the structural integrity. Furthermore, the practical numerical modelling procedure for complex composite structures under low velocity impact has been discussed.

The demonstrator structure used here was a composite lightweight bucket reinforced by multi-layered flat bed weft knitted textile preform. The bucket was subjected to five low velocity impact scenarios using a drop tower, whereas three have been discussed in detail here. The investigations showed that neither configuration led to catastrophic failure, but to local matrix cracking. The impact event has been captured via two high speed cameras, where the videos were used to obtain the local impact deformations via image correlation. This experimental procedure can be considered as a feasible and reliable way to investigate local as well as global deformation behaviour under impact loading conditions.

Considering the fiber architecture of the 3D-reinforced preform, a composite UD-material model was applied to model the impact behaviour. For the elastic impact response, an orthotropic strain rate dependency was incorporated. The modified HASHIN criterion was used to identify failure phenomena like fiber and inter-fiber failure including delamination in combination with a damage approach based on MATZENMILLER. The experimental investigations showed that the material model is capable of predicting the type, location and degree of failure. Additionally, a selective modelling approach enabled a reduction of the numerical effort of 50 %.

ACKNOWLEDGEMENTS

The authors would like to extend their gratitude to the Deutsche Forschungsgemeinschaft (DFG) for the financial support required to conduct the study within the Schwerpunktprogramm SPP 1123.

REFERENCES

- [1] Hufenbach, W.; Gude, M.; Ebert, Chr.: "Tailored 3D-textile reinforced composites with load-adapted property profiles for crash and impact applications", *Composites* 6 (2006), Nr. 3, S. 8–13
- [2] Hufenbach, W (Ed.): *Textile Verbundbauweisen und Fertigungstechnologien für Leichtbaustrukturen des Maschinen- und Fahrzeugbaus*. 2007, Progress media-Verlag, Dresden
- [3] Cherif, C.; Diestel, O.; Gries, T.: Textile Verstärkungen, Halbzeuge und deren textiltechnische Fertigung. Hufenbach, W (Ed.): *Textile Verbundbauweisen und Fertigungstechnologien für Leichtbaustrukturen des Maschinen- und Fahrzeugbaus*. 2007, Progress media-Verlag, Dresden
- [4] Cebulla, H.; Diestel, O.; Offermann, P.: "Polar Orthotropic Reinforced Weft Knitted High Performance Sphere and Helmet", *34. Int. SAMPE Tech. Conf.*, Baltimore (USA), 2002, S. 39-24
- [5] Schneider, K.; Stamm, M.: Bauteilentwicklung Schüttgutbecher. Hufenbach, W (Ed.): *Textile Verbundbauweisen und Fertigungstechnologien für Leichtbaustrukturen des Maschinen- und Fahrzeugbaus*. 2007, Progress media-Verlag, Dresden
- [6] Hufenbach, W.; Marques, F. I.; Langkamp, A.; Böhm, R.; Hornig, A.: Charpy impact tests on composite structures – An experimental and numerical investigation. *Composites Science and Technology*, 2008, Article in Press
- [7] Hufenbach, W.; Petrinic, N.; Hornig, A.; Langkamp, A.; Gude, M.; Wiegand, J.: Delamination behaviour of 3D-textile reinforced composites – Experimental and numerical approaches. *The e-Journal of Nondestructive Testing*, 1st Conference on damage in composite materials, Stuttgart, 18.-19.September 2006 11 (2006), Nr. 12
- [8] Hashin, Z.: Failure criteria for unidirectional fibre compounds. *J. App. Mech.* 47 (1980), p.329-334.
- [9] Matzenmiller, A.; Lubliner, J.; Taylor, R.L.: A constitutive model for anisotropic damage in fiber-composites. *Mech. Mater.*, Vol. 20 (1995), No. 2, p. 125-152.
- [10] Gude, M.; Ebert, C.; Langkamp, A.; Hufenbach, W.: Characterization and Simulation of the Strain Rate dependent Material Behaviour of Novel 3D Reinforced Composites. *13th European Conference on Composite Materials (ECCM 13)*, June 2-5, 2008, Stockholm, Sweden
- [11] N. N.: LS-DYNA keyword user's manual, Version 971. *Livermore Software Tech. Corp.*, 2007
- [12] Xiao, J.R.: User's manual for LS-DYNA MAT162, unidirectional and plain weave composite progressive failure models. *Center for Comp. Mat., University of Delaware, Mat. Sci. Corp.*, 2005
- [13] Zschejge, M.: Numerische und experimentelle Analyse des Impactverhaltens textilverstärkter Verbundstrukturen. *Diploma-Thesis*, TU Dresden, 2008